Electronic Supplementary Information (ESI†)

Low-Cost Synthesis of Soluble Bay-Substituted Terrylenes for p-Type Charge Transport and Efficient Photodetection on Field-Effect Transistors

Chitrak Ghosh,[‡][a] *Hayeong Park,*[‡][b] *Amrita Hazra,*[a] *Buddhadeb Mondal,*[a] *Minji Chung,*[b] *Ullrich Scherf,*[c] *Joon Hak Oh**[b] *and Suman Kalyan Samanta**[a]

[a] Department of Chemistry, Indian Institute of Technology Kharagpur, Kharagpur 721302, India.

[b] School of Chemical and Biological Engineering, Institute of Chemical Processes, Seoul National University, Seoul 08826, Republic of Korea.

[c] Macromolecular Chemistry Group (buwmakro) and Wuppertal Center for Smart Materials and Systems (CM@S), D-42119 Wuppertal, Germany

Experimental Section

Materials and methods

All the reagents, starting materials (2,3-dihydroxynaphthalene, alkyl bromides, K_2CO_3, Br_2, magnesium turnings, 1-bromo-8-chloronapthalene, $Ni(acac)_2$, and KOH), solvents and inorganic salts were purchased from commercial suppliers and were used without further purification. Solvents were dried as per literature procedure prior to use according to the requirements. Thin layer chromatography (TLC) on silica gel GF_{254} was used for the determination of R_f values, and the visualization was performed by irradiation with UV lamp at 254 nm. Column chromatography was performed on Merck silica gel (100-200 mesh) with the eluent as mentioned. ^1H (400 MHz), ^1H (500 MHz) and ^{13}C (125 MHz) NMR spectra were recorded in a Bruker 400 UltraShield and Bruker Ascend-500 NMR spectrometer in deuterated solvents at ambient temperature (300 K). Chemical shifts are reported in ppm (δ) relative to tetramethylsilane (TMS) as the internal standard ($CDCl_3$ δ 7.26 ppm for ^1H and 77.0 ppm for ^{13}C). Matrix-assisted laser desorption/ionization mass spectrometry was recorded in an Autoflex Speed LRF (Bruker) instrument. Thermogravimetric Analysis (TGA) was performed on a Pyris Diamond TG DTA (Perkin Elmer) instrument under argon with 12 °C/min heating rate. Differential scanning calorimetry was performed in a DSC25 (TA instrument) at a heating rate of 10 °C in both exothermic and endothermic scans.

Measurements of Optical Properties

UV-visible absorption spectra were recorded on a Shimadzu UV-2550 UV-vis spectrophotometer, and the fluorescence spectra were recorded on a Shimadzu RF-6000 spectrofluorometer. Fluorescence quantum yields were recorded on a Edinburgh FLS 1000 spectrofluorometer. All three compounds were taken as a solution with 10 μM concentration. For fluorescence lifetime measurement, a picoseconds diode laser (IBH, UK, Nanoled) was used as a light source at the excitation wavelength of 510 nm. The signal was detected in magic angle (54.7°) polarization using a Hamamatsu MCP PMT (3809U), and the decays were analyzed using IBH DAS-6 decay analysis software. Optical bandgaps were measured from the equation: $E_g^{opt} = 1240/\lambda_{onset}$. Absorption spectra of a thin film of the small molecules were recorded using a Cary 5000 UV-vis-NIR spectrophotometer (Agilent Technologies, Inc., USA). Thin films of the small molecules were made in a quartz plate by spin coating the 5 mg mL^{-1} solution in chloroform, followed by the optimized annealing process. The radiative and nonradiative rate (k_r and k_{nr}) were measured using equations,

$$k_r = \frac{\phi_F}{\tau}$$

$$\phi_F = \frac{k_r}{k_r + k_{nr}}$$

Cyclic Voltammetry Experiments

The electrochemical properties were characterized by a three-electrode cell with a polished 2 mm glassy carbon as the working electrode, Pt as the counter electrode, and Ag/AgCl as the reference electrode. The electrolytic solution employed was 0.1 M tetra-*n*-butylammonium perchlorate in dry dichloromethane at a scan rate of 0.1 V/s under an argon atmosphere. The reference electrode was calibrated using a ferrocene/ferrocenium redox couple as an external standard. The LUMO and HOMO energy levels of the compounds were determined by using the empirical equation,[1]

E_{LUMO} = -5.1 - [E_{red} - $E_{1/2}(Fc/Fc^+)$] eV

E_{HOMO} = -5.1 - [E_{ox} - $E_{1/2}(Fc/Fc^+)$] eV

Theoretical Calculations

The ground states of the molecules were optimized using the DFT/B3LYP method[2, 3] with the 6-31G* basis set in Gaussian 16.[4] To generate the ESP maps, Gaussview was used.[5]

Atomic Force Microscopy

AFM images of the thin films were captured using an NX-10 system (Park Systems, Korea). Thin films of the small molecules were fabricated by spin coating the 5 mg mL^{-1} solution in chloroform onto *n*-octadecyltrimethoxysilane (OTS)-modified Si/SiO_2 substrates, followed by the desired annealing process. The height and phase images were obtained in the high-resolution tapping mode under ambient conditions. The root-mean-square surface roughness (R_{RMS}) was measured from AFM topographic images (2 μm x 2 μm).

Grazing Incidence X-ray Diffraction (GIXD)

GIWAXS measurements were performed at PLS-II 9A U-SAXS beamline of Pohang Accelerator Laboratory in Korea.

OFET devices fabrication

OFETs based on the thin films of the small molecules were fabricated using heavily *n*-doped (100) silicon wafers with 300 nm thick SiO_2 (C_i = 11.5 nF cm^{-2}). The wafers were cleaned with a piranha solution for 30 min and underwent UV-ozone treatment. Subsequently, the wafer surface was treated with OTS to create a self-assembled monolayer, following a previously reported method. 5 mg mL^{-1} solution of the small molecules in chloroform was spin-coated onto the wafers at 1000 rpm for 30 s, and then annealed at the desired temperature in an N_2 environment. Subsequently, 40 nm-thick gold electrodes were thermally evaporated onto the thin films to form the source and drain electrodes using a shadow mask, with dimensions of 50 and 1,000 μm, respectively. To figure out the hole mobilities from transfer curves, the drain voltage (V_{DS}) is set to -100 V, and the gate voltage (V_{GS}) is swept from 20 V to -100 V. The electrical performances of OFETs were measured in an N_2 environment using a Keithley 4200-SCS semiconductor parametric analyzer.

Estimation of Optoelectrical Properties

To assess the phototransistor characteristics, OFET-based organic phototransistors (OPTs) were fabricated. To quantify the photosensitivity of OPTs, we calculated the photoresponsivity (R) and photo-current/dark-current ratio (p) through transfer characteristics under dark and light irradiation (λ = 532 nm, P_{max} = 79.2 mW cm^{-2}) conditions. The R and p values are typically defined by the following equations:

$$R = \frac{I_{ph}}{P_{inc}} = \frac{I_{light} - I_{dark}}{P_{inc}}$$

$$p = \frac{I_{light} - I_{dark}}{I_{dark}}$$

Where I_{ph} is the photocurrent, P_{inc} is the incident illumination power on the channel of the device, I_{light} is the drain current under illumination, and I_{dark} is the drain current in the dark. Additionally, the external quantum efficiency (EQE) (η) of OPTs was calculated, which quantifies the ratio of photogenerated carriers that effectively enhance the drain current to the number of photons incident on the OPT channel using the equation,

$$\eta = \frac{(I_{light} - I_{dark})hc}{eP_{inc}A\lambda_{peak}}$$

where h is Plank's constant, c is the speed of light, e is the fundamental unit of charge, A is the area of the transistor channel, and λ_{peak} is the peak wavelength of the incident light.

Detectivity usually indicates the smallest detectable signal, which facilitates comparisons of phototransistor devices with different configurations and areas. *D** was evaluated within this study using the equations.

$$D^* = \frac{\sqrt{A}}{NEP}$$

$$NEP = \frac{\sqrt{\overline{I_n^2}}}{R}$$

In these equations, *A* is the phototransistor active area, NEP is the noise equivalent power, and $\overline{I_n^2}$ is the measured noise current. If the major limit to detectivity is shot noise from the drain current under dark conditions, then *D** can be simplified as

$$D^* = \frac{R}{\sqrt{(2e \cdot I_{dark}/A)}}$$

Synthesis:

Compound **1** and **2** were synthesized following previous literature reports with minor modification.[6, 7]

General procedure for the Synthesis of 2,3-bis(alkyloxy)naphthalene (1a-c): DMF solution (150 mL) of 2,3-naphthalenediol (5 g, 31.2 mmol) and K_2CO_3 (43.8 g, 317 mmol) were stirred at 125 °C, then 1-bromoalkane (126.7 mmol) was added dropwise into it. The reaction mixture was stirred at 125 °C for 36 h. After that, the solution was poured into water and cooled overnight. The solid was collected and washed with MeOH, to obtain the product as white solids.

Compound **1a:** Yield 97%. ^{1}H NMR (500 MHz, $CDCl_3$) δ 7.65 (dd, *J* = 6.1, 3.3 Hz, 2H), 7.30 (dd, *J* = 6.1, 3.2 Hz, 2H), 7.12 (s, 2H), 4.11 (t, 4H), 1.96 – 1.84 (m, 4H), 1.56 – 1.46 (m, 4H), 1.42 – 1.28 (m, 16H), 0.90 (t, 6H). ^{13}C NMR (125 MHz, $CDCl_3$) δ 149.67, 129.44, 126.35, 124.06, 108.12, 69.06, 31.99, 29.55, 29.44, 29.29, 26.25, 22.83, 14.24.

Compound **1b:** Yield 95%. ^{1}H NMR (500 MHz, $CDCl_3$) δ 7.65 (dd, *J* = 6.1, 3.3 Hz, 2H), 7.30 (dd, *J* = 6.1, 3.2 Hz, 2H), 7.12 (s, 2H), 4.11 (t, 4H), 1.94 – 1.84 (m, 4H), 1.56 – 1.48 (m, 4H), 1.41 – 1.25 (m, 32H), 0.89 (t, 6H). ^{13}C NMR (125 MHz, $CDCl_3$) δ 149.67, 129.44, 126.35, 124.06, 108.13, 69.06, 32.08, 29.86, 29.82, 29.80, 29.60, 29.52, 29.29, 26.25, 22.84, 14.25.

Compound **1c:** Yield 90%. ^{1}H NMR (500 MHz, $CDCl_3$) δ 7.65 (dd, *J* = 6.1, 3.3 Hz, 2H), 7.30 (dd, *J* = 6.1, 3.2 Hz, 2H), 7.11 (s, 2H), 4.11 (t, 4H), 1.93 – 1.85 (m, 4H), 1.54 – 1.49 (m, 4H), 1.28 (m, 48H), 0.88 (t, 6H). ^{13}C NMR (125 MHz, $CDCl_3$) δ 149.67, 129.44, 126.36, 124.06, 108.12, 69.06, 32.09, 29.87, 29.82, 29.80, 29.60, 29.52, 29.29, 26.25, 22.84, 14.25.

General procedure for the Synthesis of 1,4-dibromo-2,3-bis(alkyloxy)naphthalene (2a-c): Bromine (2.1 equivalent) in dichloromethane was added into the stirred solution of 2,3-bis(alkyloxy)naphthalene (**1**) in DCM and the mixture was stirred at room temperature for 15 minutes. After that, the excess bromine was quenched with sodium thiosulfate solution in water. Then, the product was extracted from DCM, washed with water and brine, and dried over Na_2SO_4 and then precipitated in cold methanol to get the pure product as white solid.

Compound **2a:** Yield 90%. ^{1}H NMR (500 MHz, $CDCl_3$) δ 8.24 (dd, *J* = 6.4, 3.3 Hz, 2H), 7.55 (dd, *J* = 6.5, 3.3 Hz, 2H), 4.12 (t, 4H), 1.92 – 1.84 (m, 4H), 1.55 – 1.50 (m, 4H), 1.41 – 1.27 (m, 16H), 0.90 (t, 6H). ^{13}C NMR (125 MHz, $CDCl_3$) δ 150.27, 130.33, 127.41, 127.08, 116.55, 74.62, 32.01, 30.46, 29.62, 29.45, 26.26, 22.82, 14.24.

Compound **2b:** Yield 87%. ^{1}H NMR (500 MHz, $CDCl_3$) δ 8.24 (dd, *J* = 6.4, 3.2 Hz, 2H), 7.54 (dd, *J* = 6.4, 3.3 Hz, 2H), 4.12 (t, 4H), 1.94 – 1.79 (m, 4H), 1.53 (d, 4H), 1.43 – 1.20 (m, 32H), 0.88 (t, 6H). ^{13}C NMR (125 MHz, $CDCl_3$) δ 150.27, 130.33, 127.42, 127.08, 116.55, 74.62, 32.09, 30.46, 29.85, 29.81, 29.66, 29.52, 26.26, 22.85, 14.25.

Compound **2c:** Yield 86%. ^{1}H NMR (400 MHz, $CDCl_3$) δ 8.24 (dd, *J* = 6.4, 3.2 Hz, 2H), 7.54 (dd, *J* = 6.4, 3.2 Hz, 2H), 4.12 (t, 4H), 1.93 – 1.83 (m, 4H), 1.58 – 1.49 (m, 4H), 1.42 – 1.19 (m, 48H), 0.88 (t, 6H). ^{13}C NMR (125 MHz, $CDCl_3$) δ 150.28, 130.34, 127.42, 127.08, 116.55, 74.62, 32.09, 30.46, 29.88, 29.86, 29.83, 29.81, 29.67, 29.53, 26.27, 22.85, 14.25.

General procedure for the synthesis of 8,8''-dichloro-2',3'-bis(alkyloxy)-1,1',4,1''-ternaphthalene (3a-c): Under an argon atmosphere, a mixture of magnesium turnings (68 mmol) and 10 mL of dry THF in an oven-dried flask was stirred at 50 °C and 0.2 mL of 1,2-dibromoethane was added. The mixture was continued heating at 50 °C over a period of 10 minutes and a solution of 1,4-dibromo-2,3-bis(alkyloxy)naphthalene (**2**, 6.78 mmol) in 10 mL of dry THF was added slowly through a syringe. The solution was stirred for one hour at 50 °C to obtain a greyish transparent solution, which was kept carefully for the next step. In another two-neck round bottom flask, 1-bromo-8-chloronaphthalene (13.58 mmol) and $Ni(acac)_2$ (0.135 mmol) were dissolved in 10 mL dry THF and the Grignard reagent was introduced at

room temperature under argon atmosphere. The mixture was stirred at room temperature for one hour and then acidified with 2N HCl. The product was extracted from $CHCl_3$, washed with water and brine, and dried over Na_2SO_4. The filtrate was evaporated and the compound was purified by column chromatography on silica gel (hexane/chloroform 9:1) to give compounds **3a-c** as a pale-yellow solid.

Compound **3a:** Yield 37%. ^{1}H NMR (400 MHz, $CDCl_3$) δ 7.91 (d, *J* = 8.1 Hz, 2H), 7.83 (d, *J* = 8.1 Hz, 2H), 7.56 (t, *J* = 7.6 Hz, 2H), 7.49 (d, *J* = 7.0 Hz, 2H), 7.41 (d, *J* = 7.3 Hz, 2H), 7.31 (t, *J* = 7.7 Hz, 2H), 7.20 (dd, *J* = 8.1, 5.1 Hz, 2H), 7.11 (dd, *J* = 6.4, 3.3 Hz, 2H), 3.85 (dt, 2H), 3.78 – 3.68 (m, 2H), 1.23 – 1.07 (m, 8H), 1.05 – 0.95 (m, 4H), 0.94 – 0.85 (m, 4H), 0.79 (t, 10H), 0.63 – 0.51 (m, 4H). ^{13}C NMR (125 MHz, $CDCl_3$) δ 149.19, 136.19, 133.63, 133.22, 132.45, 131.57, 131.54, 130.49, 129.35, 129.18, 128.58, 126.28, 125.83, 125.55, 124.49, 77.41, 77.16, 76.91, 72.57, 31.86, 30.28, 29.29, 29.22, 25.68, 22.79, 14.23. MALDI-ToF- Calculated (m/z): 704.3188; obtained (m/z): 704.9735.

Compound **3b:** Yield 32%. ^{1}H NMR (400 MHz, $CDCl_3$) δ 7.91 (d, J = 8.1 Hz, 2H), 7.83 (d, J = 8.1 Hz, 2H), 7.56 (t, J = 7.6 Hz, 2H), 7.49 (d, J = 7.0 Hz, 2H), 7.41 (d, J = 7.3 Hz, 2H), 7.31 (t, J = 7.7 Hz, 2H), 7.20 (dd, J = 8.1, 5.1 Hz, 2H), 7.11 (dd, J = 6.4, 3.3 Hz, 2H), 3.85 (dt, 2H), 3.78 – 3.68 (m, 2H), 1.23 – 1.07 (m, 8H), 1.05 – 0.95 (m, 4H), 0.94 – 0.85 (m, 4H), 0.79 (t, 10H), 0.63 – 0.51 (m, 4H). ^{13}C NMR (125 MHz, $CDCl_3$) δ 149.21, 136.20, 133.66, 133.23, 132.46, 131.60, 131.56, 130.51, 129.36, 129.18, 128.58, 126.29, 125.84, 125.55, 124.49, 72.58, 32.11, 30.29, 29.84, 29.82, 29.67, 29.59, 29.54, 29.35, 25.70, 22.86, 14.26. MALDI-ToF- Calculated (m/z): 816.4440; obtained (m/z): 817.2237.

Compound **3c:** Yield 30%. ^{1}H NMR (400 MHz, $CDCl_3$) δ 7.99 (d, *J* = 8.0 Hz, 2H), 7.91 (d, *J* = 8.0 Hz, 2H), 7.63 (t, *J* = 7.6 Hz, 2H), 7.56 (d, *J* = 6.9 Hz, 2H), 7.49 (d, *J* = 7.3 Hz, 2H), 7.39 (t, *J* = 7.7 Hz, 2H), 7.27 (dd, *J* = 6.6, 3.5 Hz, 2H), 7.18 (dd, *J* = 6.5, 3.2 Hz, 2H), 3.92 (dt, 2H), 3.80 (dd, 2H), 1.32 – 1.14 (m, 40H), 1.09 (dd, 4H), 0.95 (dd, 4H), 0.89 (t, 10H), 0.65 (dt, 4H). ^{13}C NMR (125 MHz, $CDCl_3$) δ 149.20, 136.19, 133.65, 133.23, 132.46, 131.59, 131.55, 130.50, 129.36, 129.18, 128.58, 126.28, 125.84, 125.55, 124.49, 72.57, 32.09, 30.29, 29.89, 29.88, 29.85, 29.84, 29.68, 29.60, 29.53, 29.36, 25.70, 22.85, 14.25. MALDI-ToF- Calculated (m/z): 928.5692; obtained (m/z): 929.6367.

General procedure for the Synthesis of 7,8-bis(hexadecyloxy)terrylene (4a-c): A solution of compound **3** (0.284 mmol) and excess KOH (260 mmol) in distilled quinoline (2 mL) was

heated at 195 ºC under an argon atmosphere for 4 hours. After cooling to room temperature, the product was extracted with chloroform. The organic layer was washed with hydrochloric acid, water, and brine and dried over Na_2SO_4. The filtrate was evaporated and purified by column chromatography on silica gel (hexane/chloroform 9:1) to give compounds **4a-c** as a deep purple solid.

Compound **4a:** Yield 62%. ^{1}H NMR (500 MHz, $CDCl_3$) δ 9.29 (d, *J* = 7.7 Hz, 2H), 8.24 (s, 1H), 8.20 (d, *J* = 7.5 Hz, 2H), 7.72 (dd, *J* = 7.8, 2.5 Hz, 4H), 7.52 (q, *J* = 8.0 Hz, 4H), 4.09 (t, 4H), 1.99 – 1.92 (m, 4H), 1.43 – 1.25 (m, 20H), 0.90 (t, 6H). ^{13}C NMR (125 MHz, $CDCl_3$) δ 152.36, 134.40, 131.34, 130.30, 130.10, 129.19, 128.16, 127.70, 126.94, 126.72, 126.38, 123.53, 121.02, 120.04, 73.02, 32.01, 30.86, 29.74, 29.48, 26.43, 22.84, 14.24. MALDI-ToF- Calculated (m/z): 632.3654; obtained (m/z): 633.1290.

Compound **4b:** Yield 60%. ^{1}H NMR (400 MHz, $CDCl_3$) δ 9.29 (d, *J* = 7.6 Hz, 2H), 8.23 (s, 2H), 8.20 (d, *J* = 7.3 Hz, 2H), 7.71 (d, *J* = 7.7 Hz, 4H), 7.52 (dd, *J* = 14.3, 7.5 Hz, 4H), 4.08 (t, 4H), 2.00 – 1.88 (m, 4H), 1.57 – 1.48 (m, 4H), 1.43 – 1.22 (m, 32H), 0.89 (t, 6H). ^{13}C NMR (125 MHz, $CDCl_3$) δ 152.37, 134.40, 131.34, 130.31, 130.10, 129.19, 128.17, 127.71, 126.95, 126.72, 126.38, 123.53, 121.03, 120.04, 73.02, 32.10, 30.86, 29.88, 29.84, 29.82, 29.78, 29.54, 26.43, 22.85, 14.25. MALDI-ToF- Calculated (m/z): 744.4906; obtained (m/z): 745.2999.

Compound **4c:** Yield 53%. ^{1}H NMR (500 MHz, $CDCl_3$) δ 9.28 (d, *J* = 7.3 Hz, 2H), 8.23 (s, 2H), 8.19 (d, *J* = 7.3 Hz, 2H), 7.71 (dd, *J* = 7.9, 3.0 Hz, 4H), 7.52 (dd, *J* = 16.8, 8.0 Hz, 4H), 4.09 (t, 4H), 1.99 – 1.91 (m, 4H), 1.55 – 1.49 (m, 4H), 1.41 – 1.26 (m, 48H), 0.88 (t, 6H). ^{13}C NMR (125 MHz, $CDCl_3$) δ 152.38, 134.41, 131.35, 130.32, 130.11, 129.20, 128.18, 127.72, 126.96, 126.73, 126.39, 123.54, 121.03, 120.04, 73.03, 32.09, 30.86, 29.89, 29.85, 29.84, 29.82, 29.78, 29.53, 29.51, 26.43, 22.84, 14.24. MALDI-ToF- Calculated (m/z): 856.6158; obtained (m/z): 857.6020.

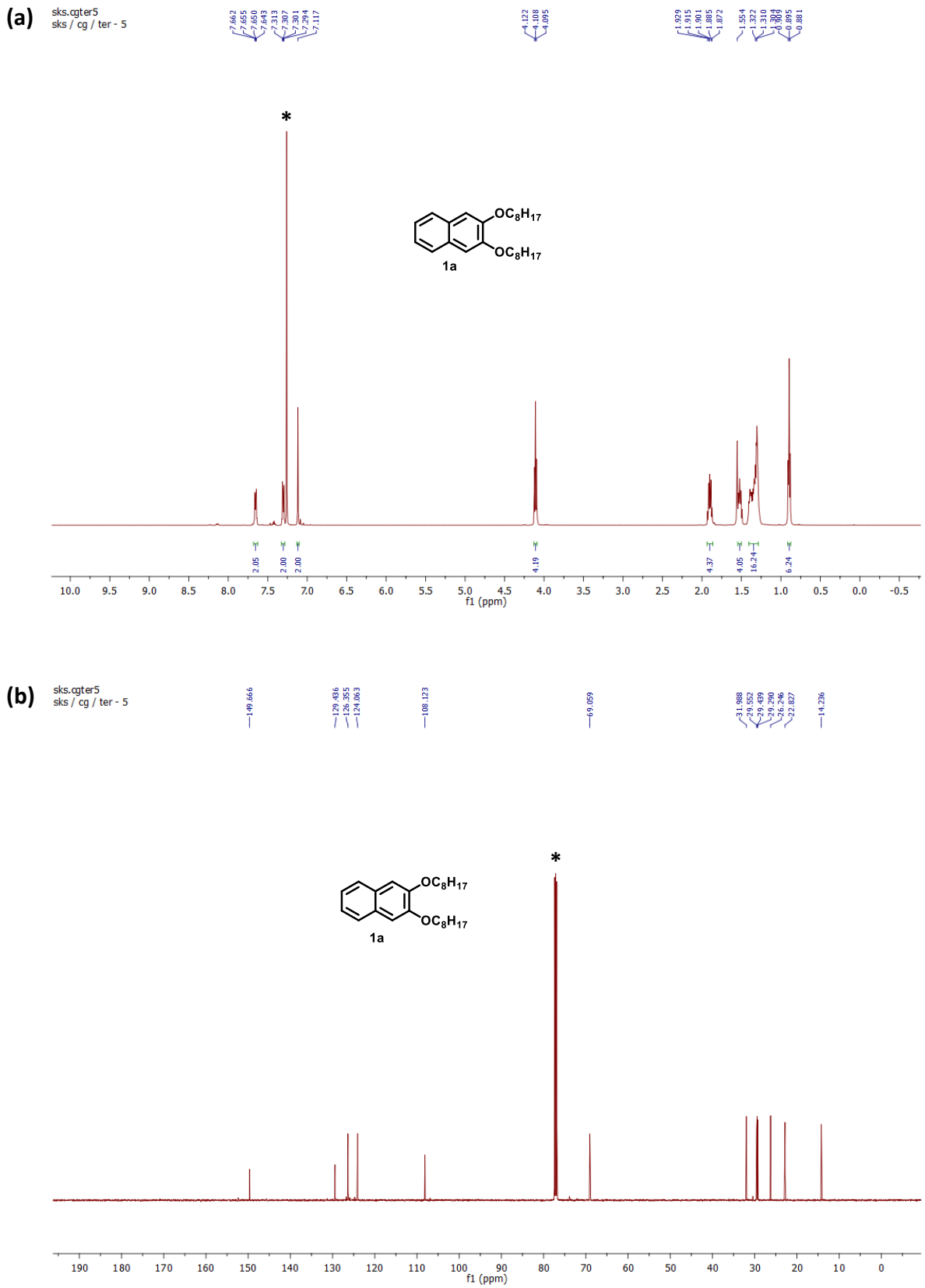

Fig. S1. (a) ^{1}H and (b) ^{13}C NMR spectra of **1a** in $CDCl_3$ (*) at 298K.

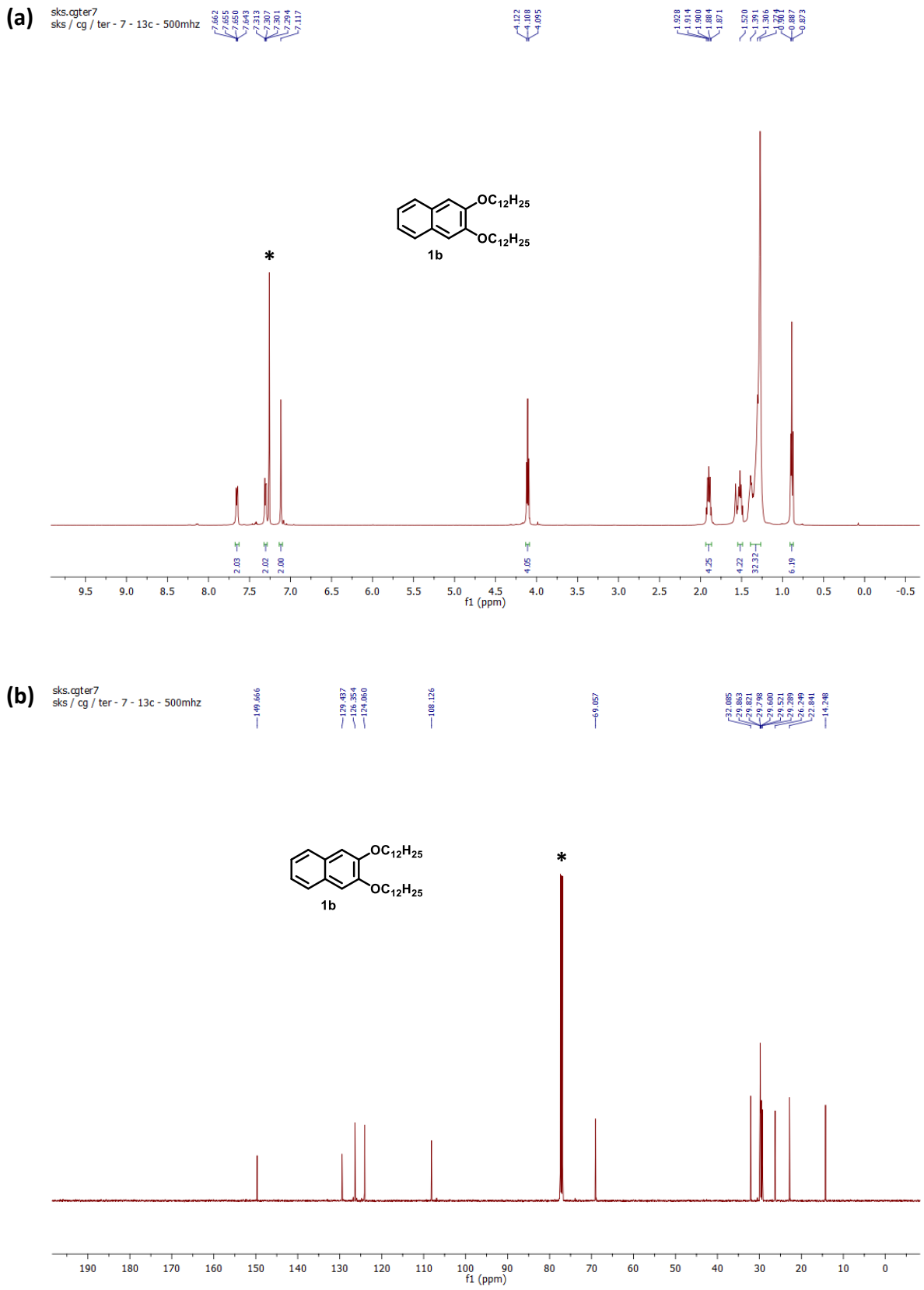

Fig. S2. (a) ^{1}H and (b) ^{13}C NMR spectra of **1b** in $CDCl_3$ (*) at 298K.

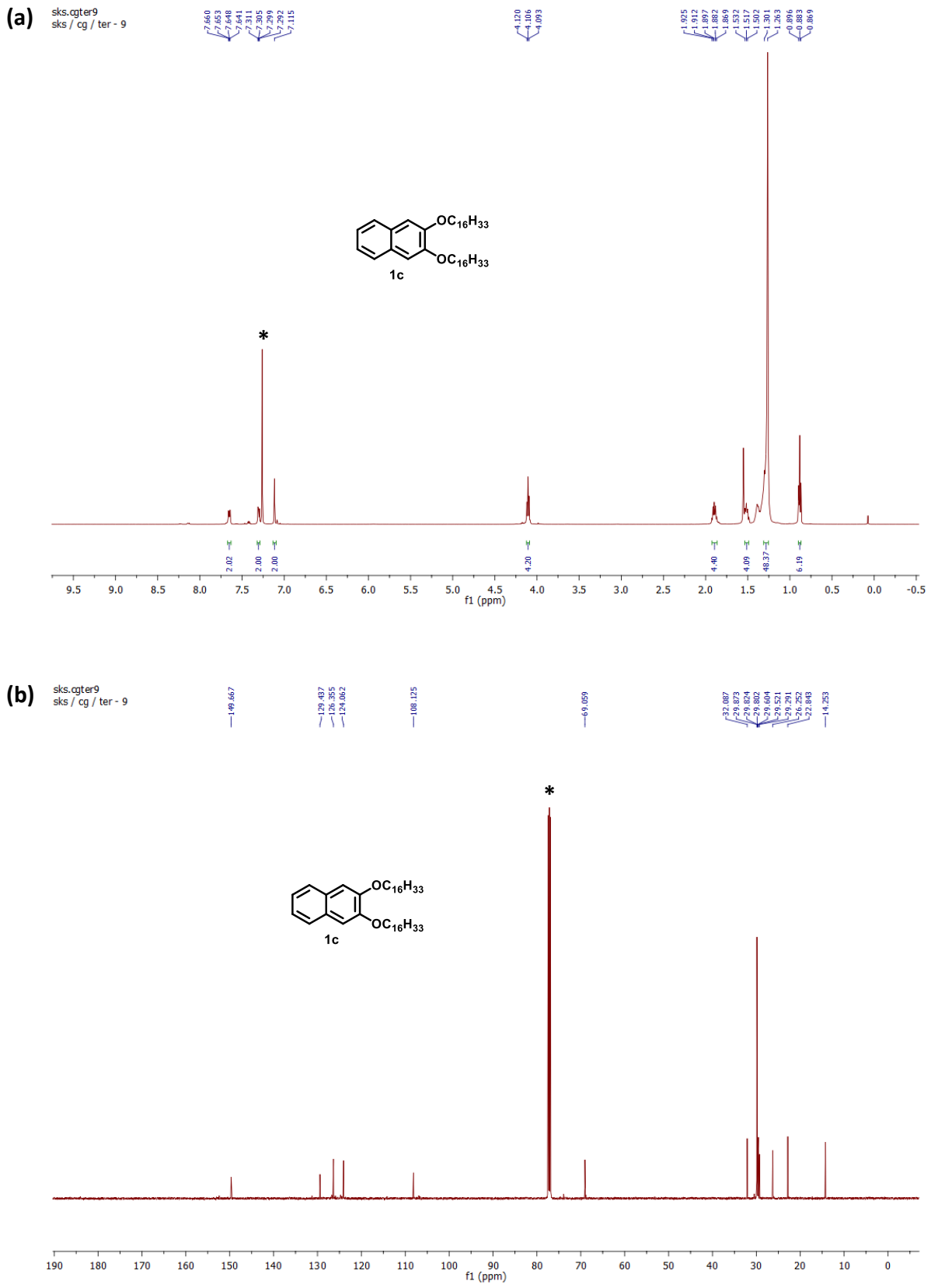

Fig. S3. (a) ^{1}H and (b) ^{13}C NMR spectra of **1c** in $CDCl_3$ (*) at 298K.

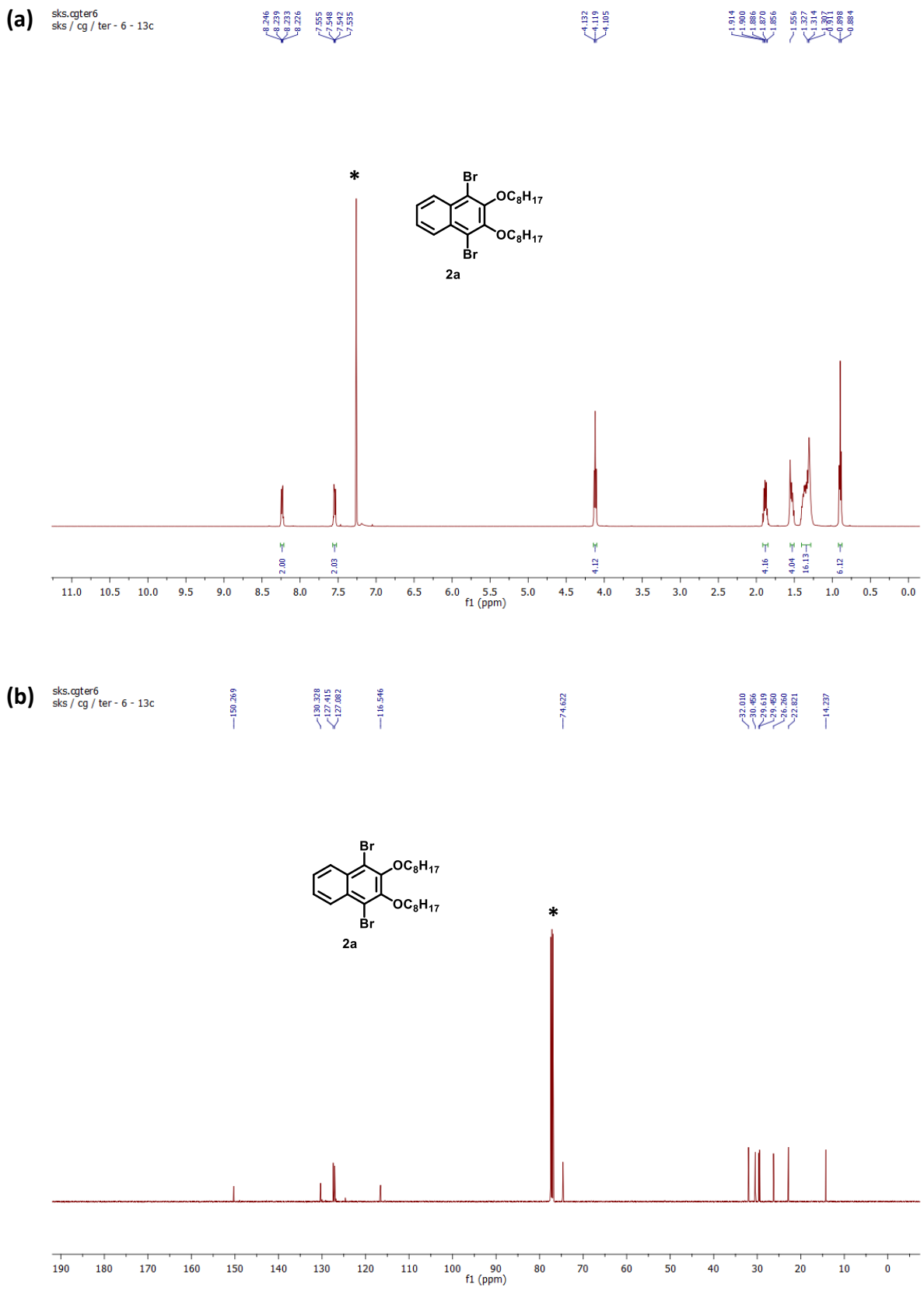

Fig. S4. (a) ^{1}H and (b) ^{13}C NMR spectra of **2a** in $CDCl_3$ (*) at 298K.

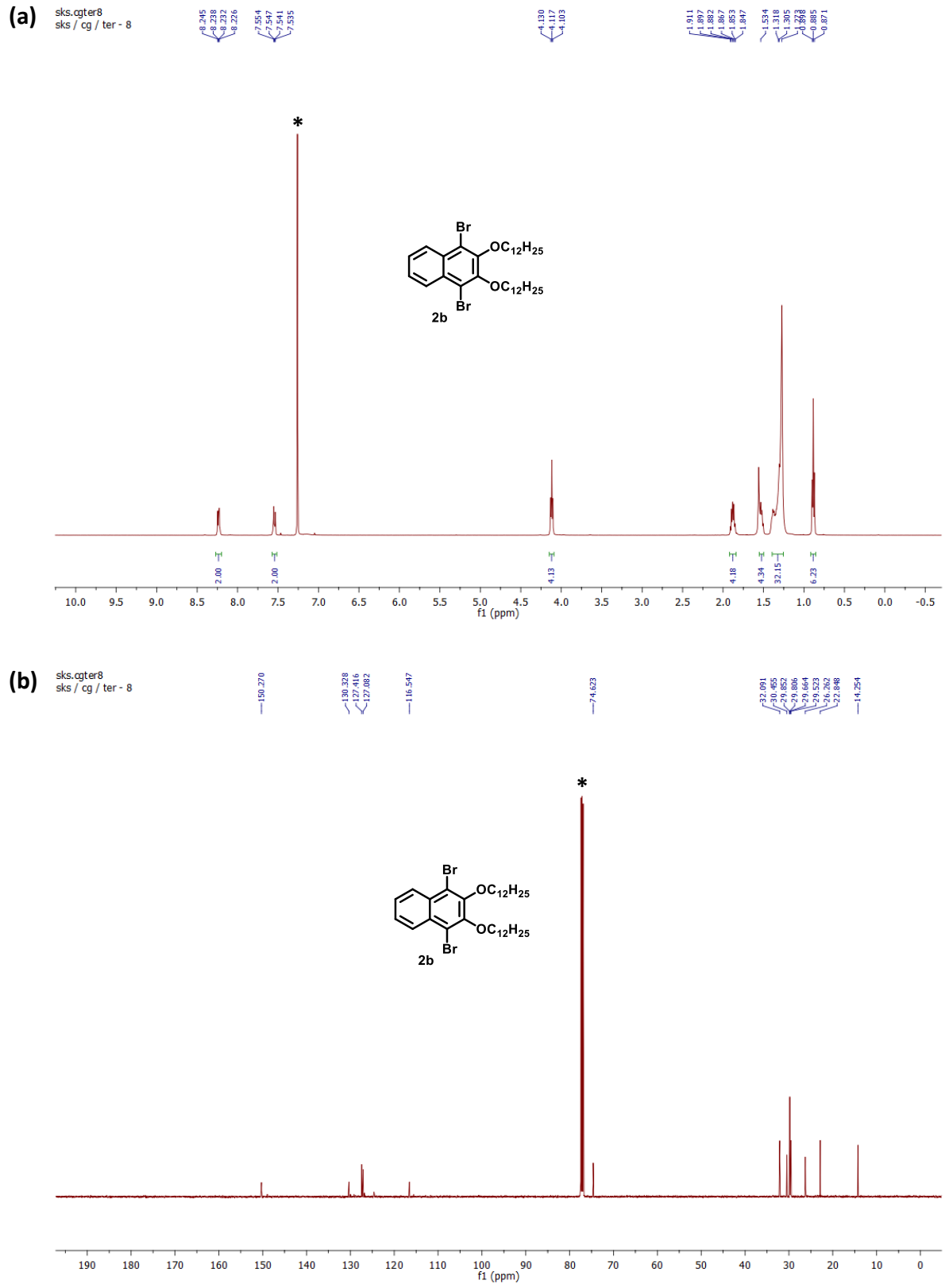

Fig. S5. (a) ^{1}H and (b) ^{13}C NMR spectra of **2b** in $CDCl_3$ (*) at 298K.

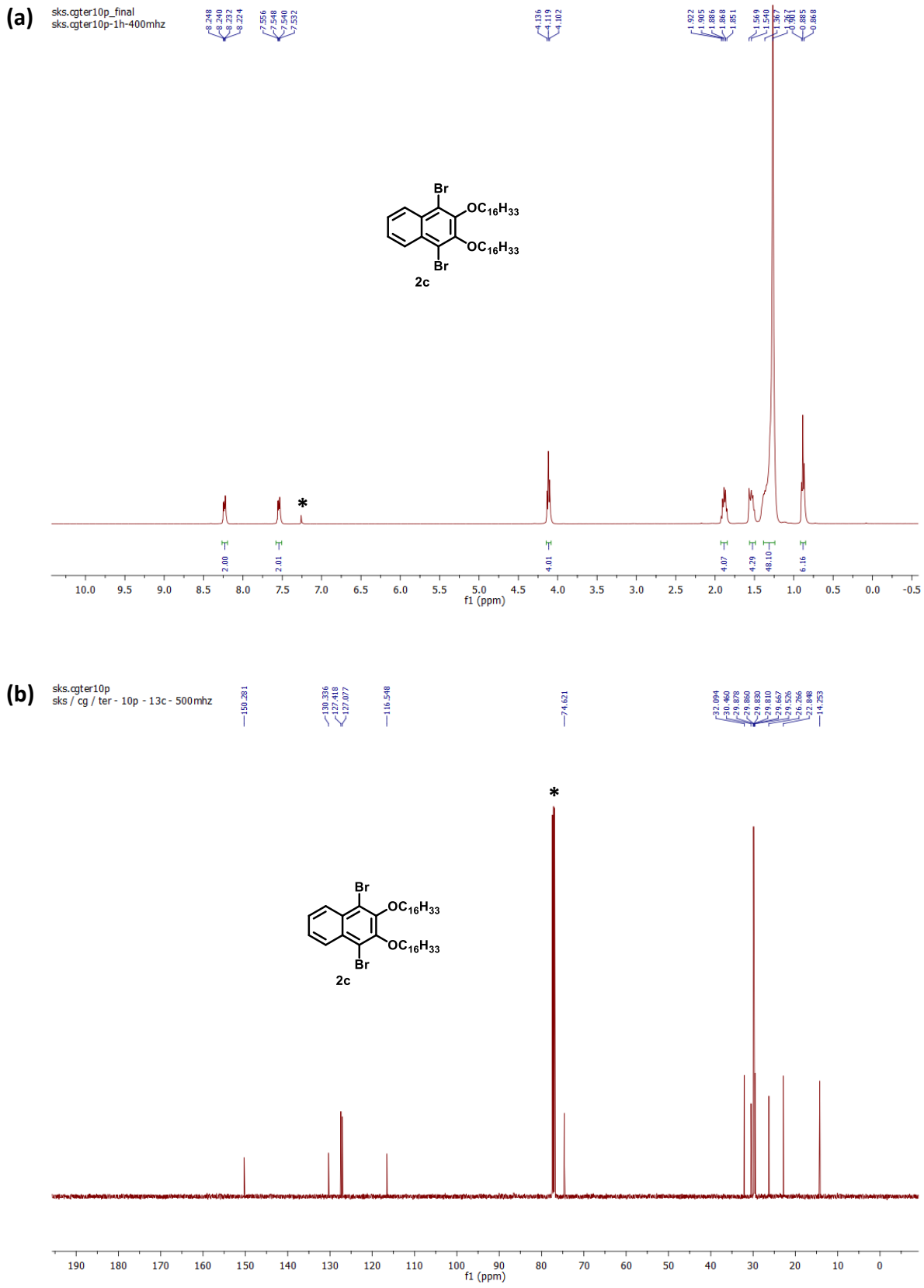

Fig. S6. (a) ^{1}H and (b) ^{13}C NMR spectra of **2c** in $CDCl_3$ (*) at 298K.

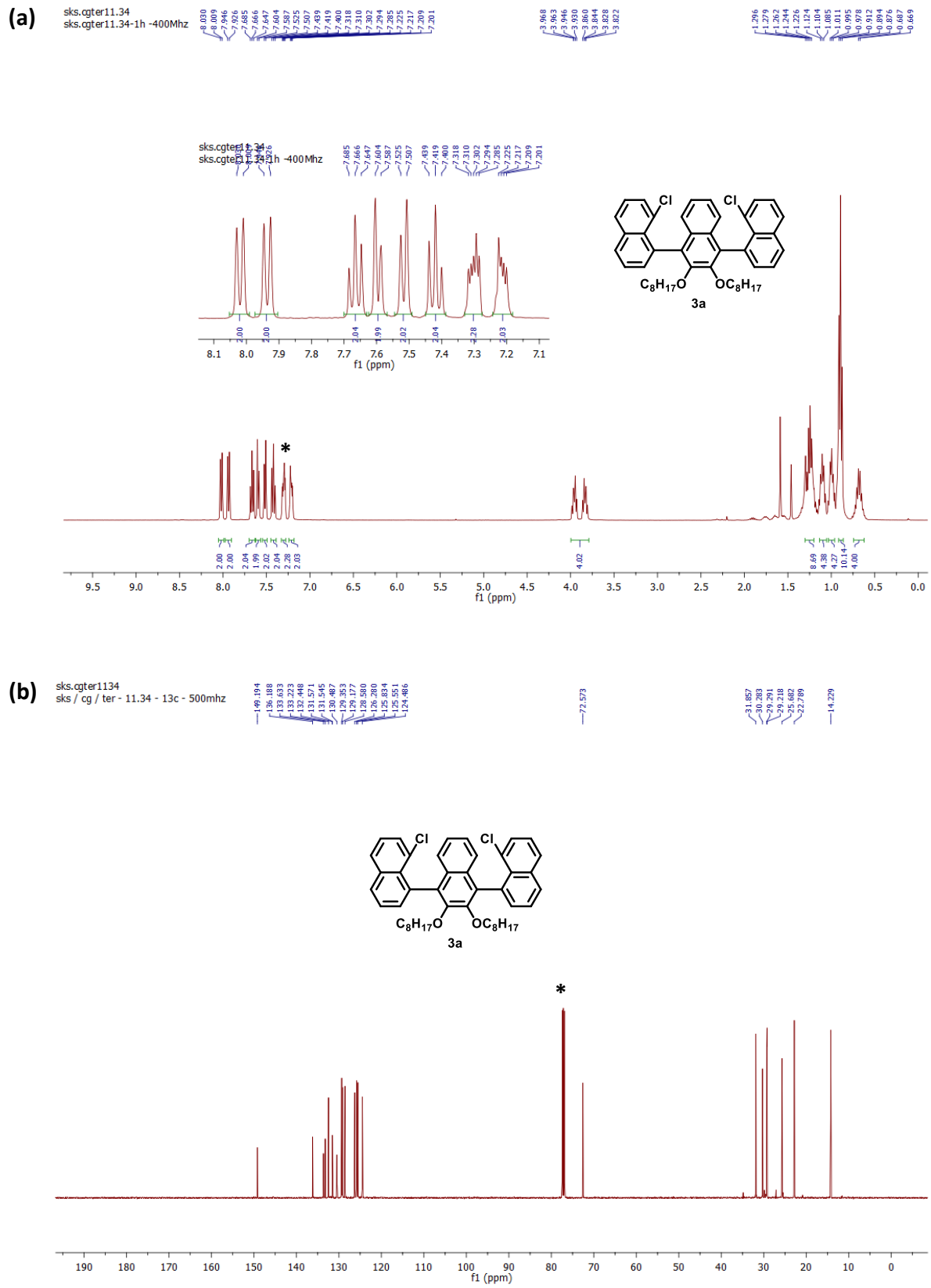

Fig. S7. (a) ^{1}H and (b) ^{13}C NMR spectra of **3a** in $CDCl_3$ (*) at 298K.

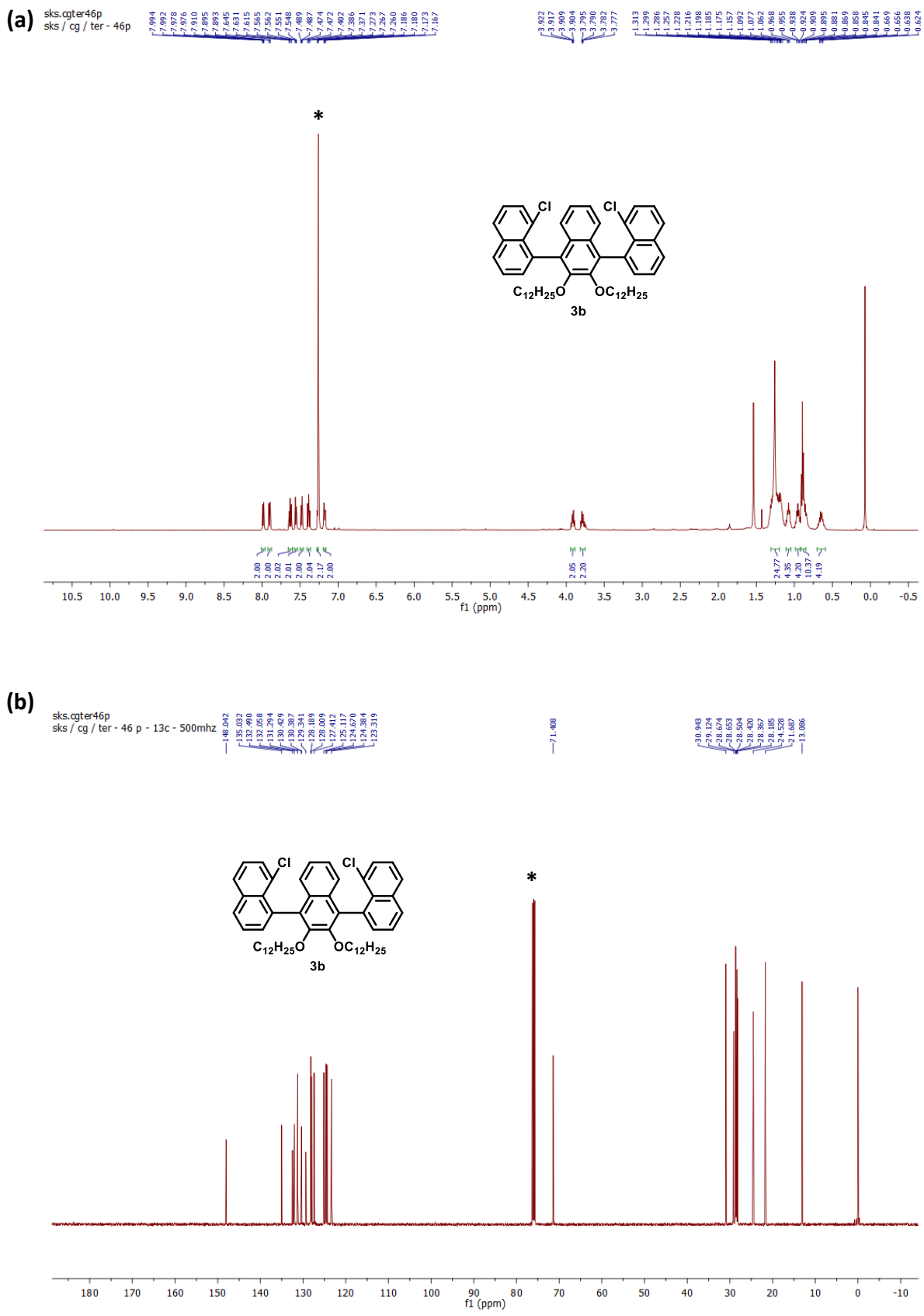

Fig. S8. (a) ^{1}H and (b) ^{13}C NMR spectra of **3b** in $CDCl_3$ (*) at 298K.

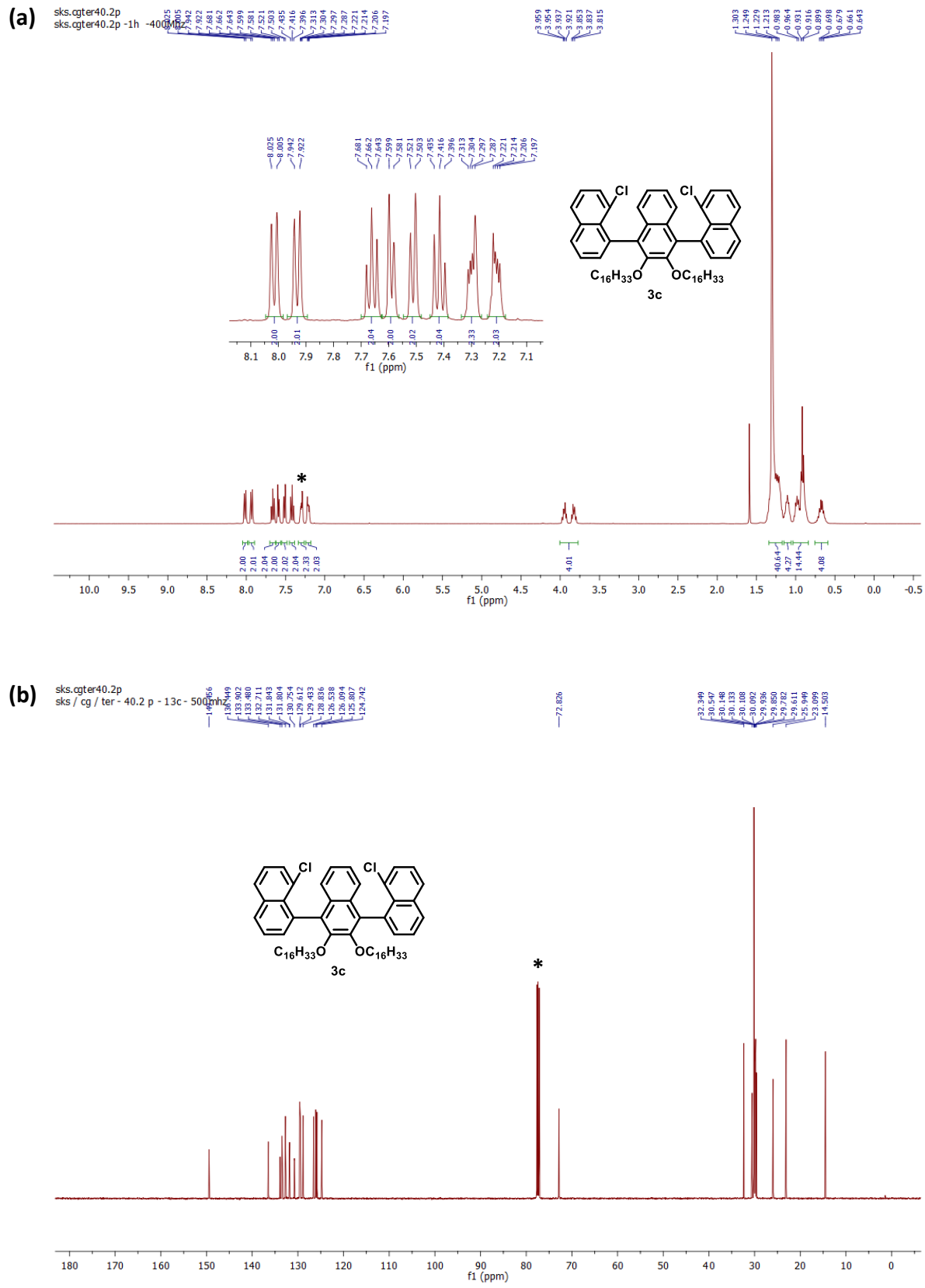

Fig. S9. (a) ^{1}H and (b) ^{13}C NMR spectra of **3c** in $CDCl_3$ (*) at 298K.

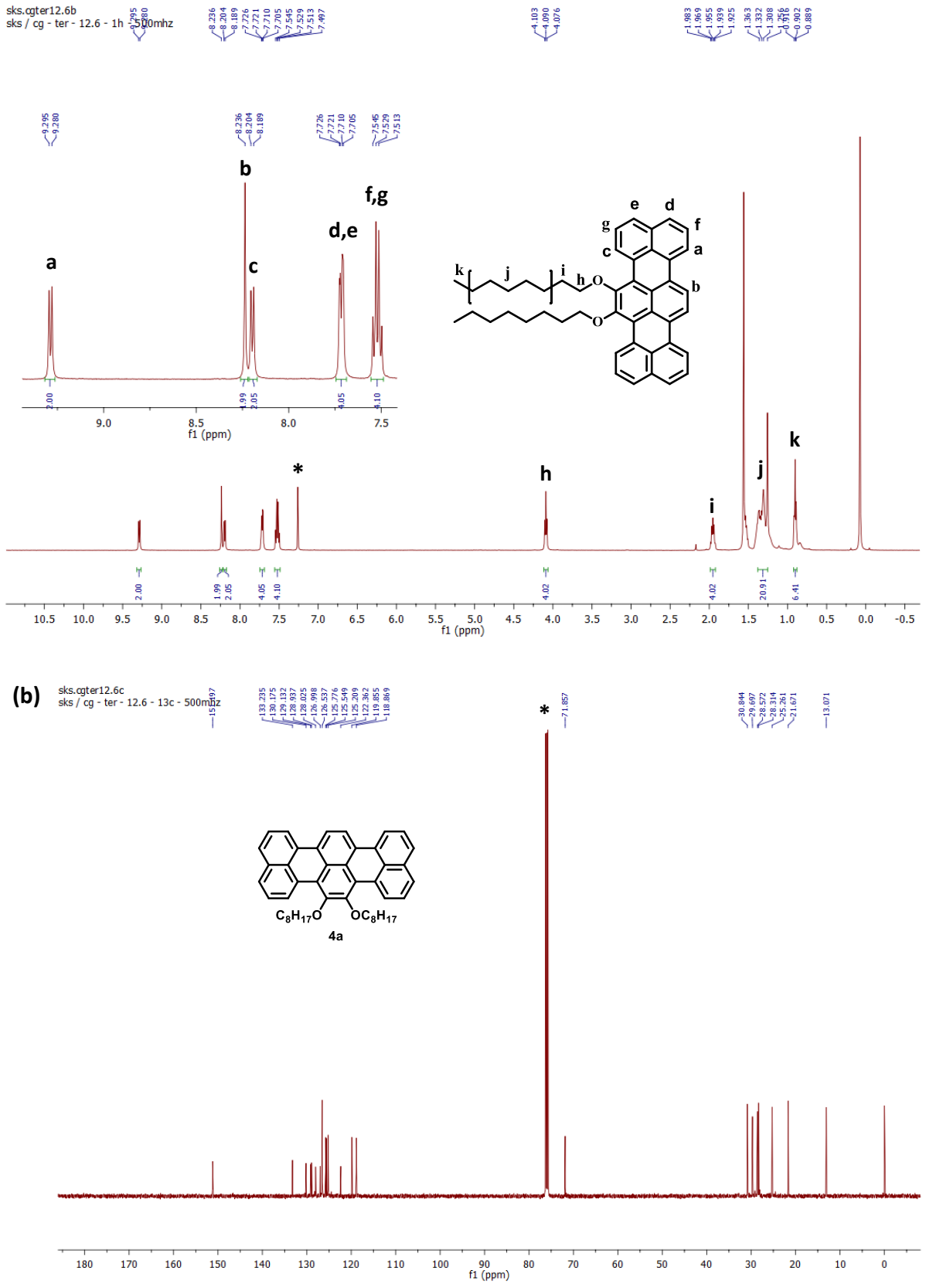

Fig. S10. (a) ^{1}H and (b) ^{13}C NMR spectra of **TER-C8** (**4a**) in $CDCl_3$ (*) at 298K.

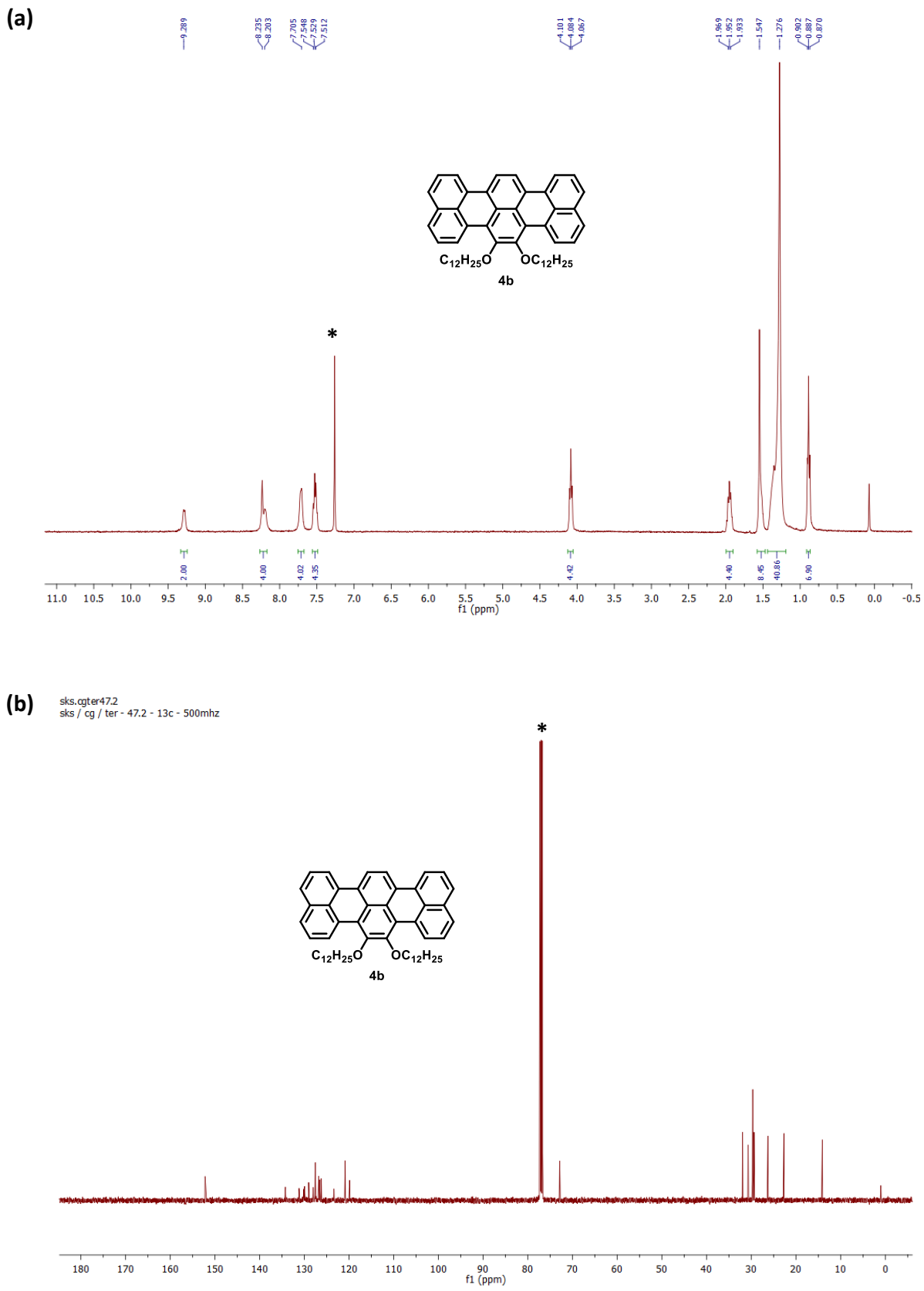

Fig. S11. (a) ^{1}H and (b) ^{13}C NMR spectra of **TER-C12** (**4b**) in $CDCl_3$ (*) at 298K.

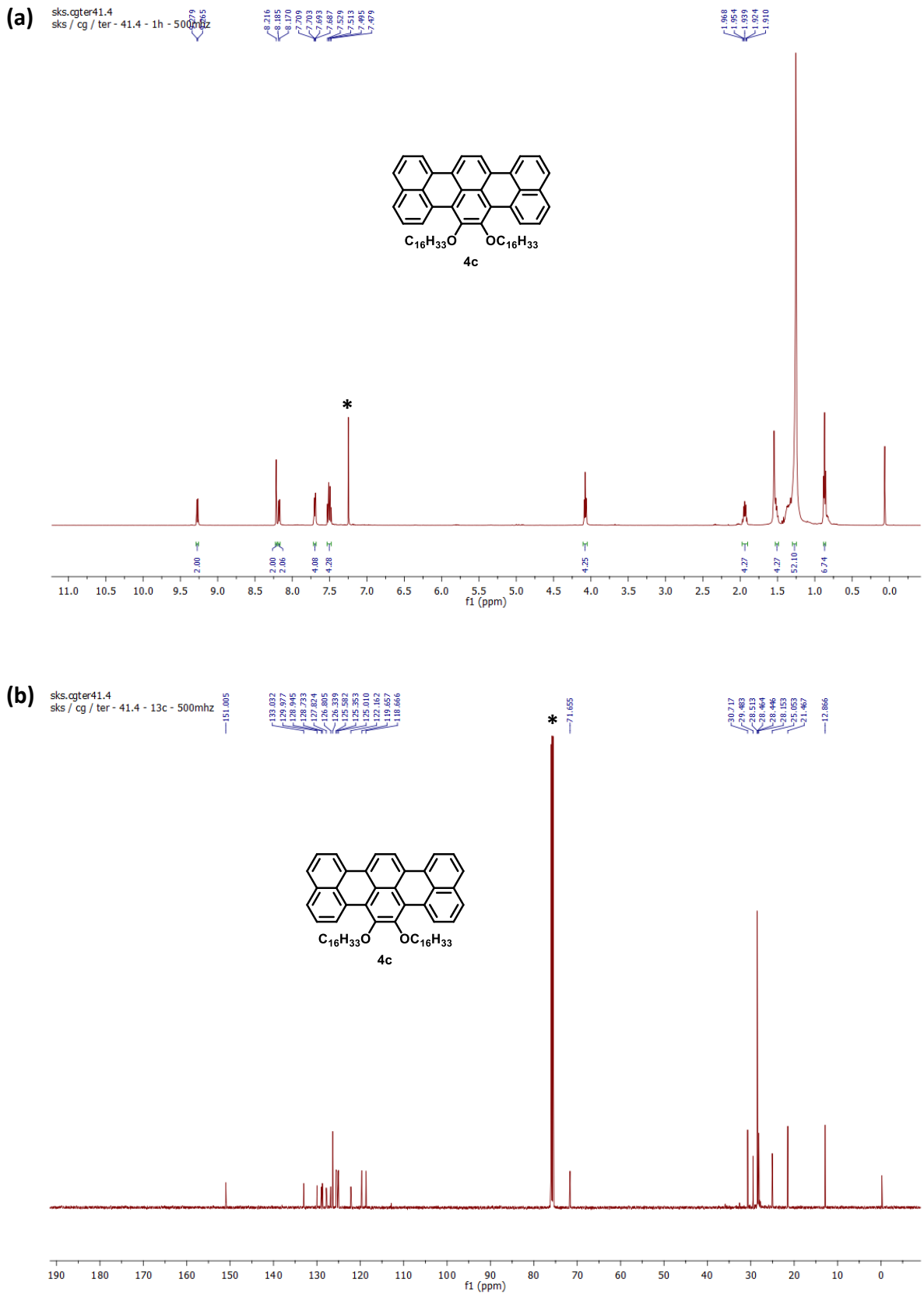

Fig. S12. (a) ^{1}H and (b) ^{13}C NMR spectra of **TER-C16** (**4c**) in $CDCl_3$ (*) at 298K.

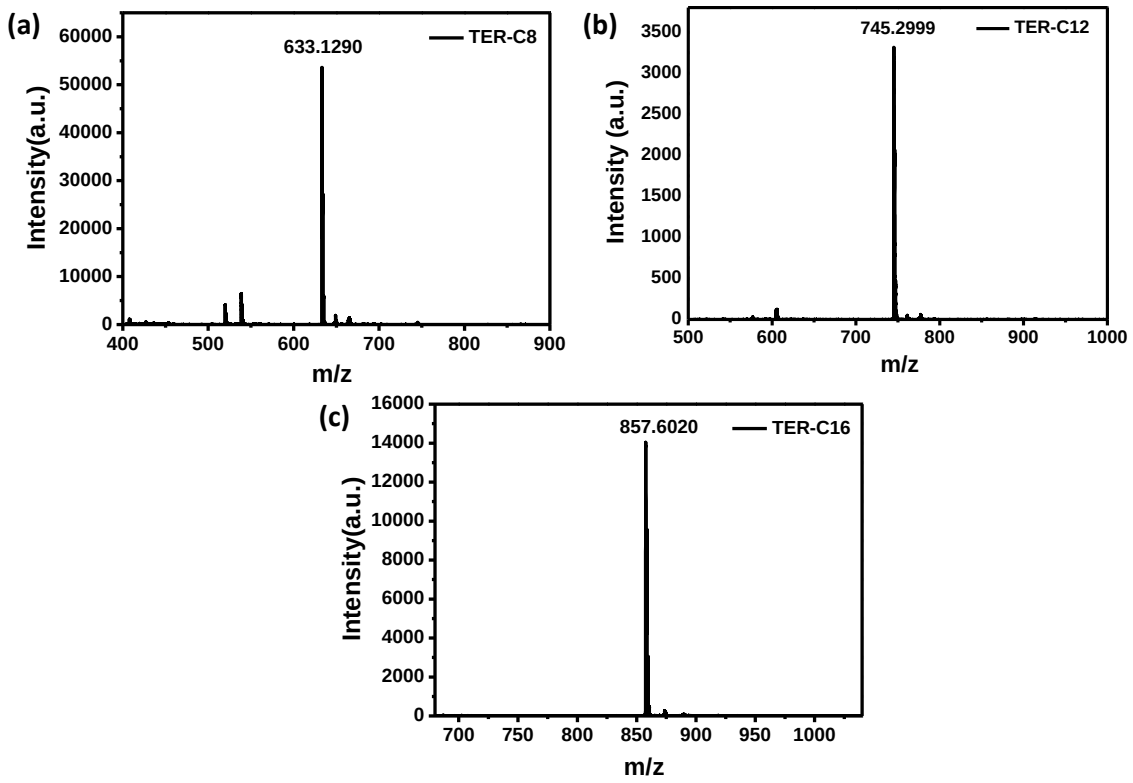

Fig. S13. MALDI-ToF spectra of (a)**TER-C8**, (b) **TER-C12** and (c) **TER-C16**.

Cost Analysis for Synthesizing 1g of TER-C8.

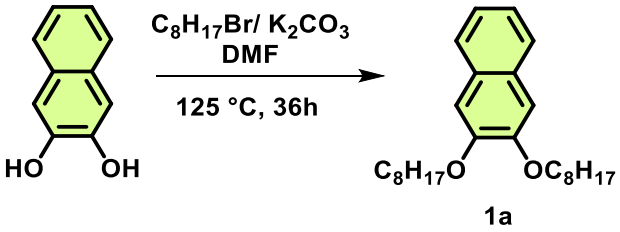

Table S1. Estimated cost of synthesis of intermediate **1a**.

Chemicals	**Supplier**	**Price ($)**	**Reagents required for batch preparation**	**Total cost ($)**
2,3-dihydroxynaphthalene	Alfa Aesar	0.66 $/g	1 g	0.66
K_2CO_3	SRL	0.01 $/g	8.6 g	0.086
DMF	SRL	10.6 $/L	20 ml	0.212
$C_8H_{17}Br$	SRL	90 $/L	2.8 ml	0.252
Total Cost				**1.21**

Yield = 2.3 g, Cost of 1g of 1a is 0.52 $

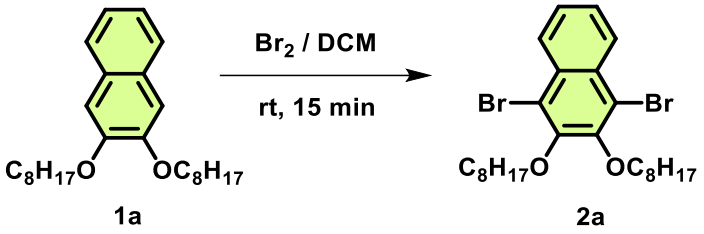

Table S2. Estimated cost of synthesis of intermediate **2a**.

Chemicals	Supplier	Price ($)	Reagents required for batch preparation	Total cost ($)
1a		0.52 $/g	1 g	0.52
Bromine	Spectrochem	113 $/L	0.28 mL	0.03
DCM	Local	8 $/L	50 ml	0.4
Total Cost				**0.95**

Yield = 1.27 g, Cost of 1g of 2a is 0.75 $.

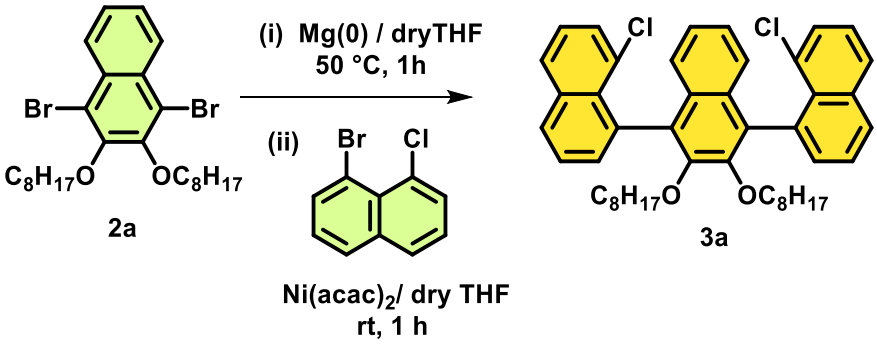

Table S3. Estimated cost of synthesis of intermediate **3a**.

Chemicals	Supplier	Price ($)	Reagents required for batch preparation	Total cost ($)
2a		0.75 $/g	1 g	0.75
1-bromo-8-choloronaphthalene	BLD Pharm	3.5 $/g	0.9 g	3.15
Mg turnings	Sigma	0.26 $/g	0.45 g	0.12
$Ni(acac)_2$	Sigma	5.4 $/g	0.012 g	0.06
THF	Finar	15 $/L	15 ml	0.1
Silica gel	Local	17 $/kg	80 g	1.36
Petroleum ether	Local	5 $/L	300 ml	1.6
$CHCl_3$	Finar	8 $/L	50 ml	0.4
Total				7.54

Yield = 0.48 g, Cost of 1 g of 4a is 15.7 $

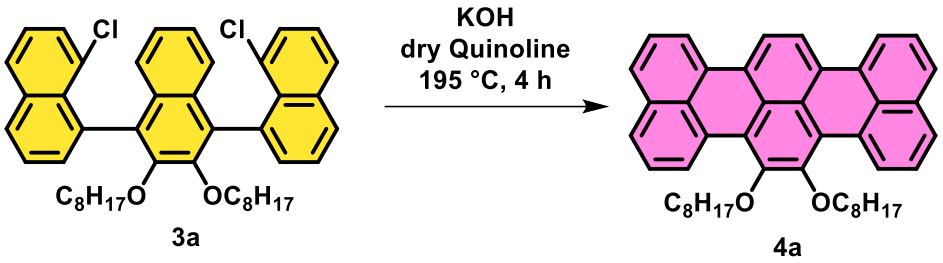

Table S4. Estimated cost of synthesis of intermediate **3a**.

Chemicals	Supplier	Price ($)	Reagents required for batch preparation	Total cost ($)
3a		15.7 $/g	200 mg	3.14
KOH	SRL	0.012 $/g	15 g	0.18
Quinoline	SRL	43.5 $/L	2 mL	0.09
Silica gel	Local	17 $/kg	80 g	1.36
Petroleum ether	Local	5 $/L	300 ml	1.6
$CHCl_3$	Finar	8 $/L	50 ml	0.4
Total				6.77

Yield = 0.11 g, Cost of 1g of 5a is 61.5 $

Table S5. Cost comparison between commercially available unsubstituted terylene and our synthesized **TER-C8**.

Chemicals	Supplier	Price ($)
Terrylene	Alfa Chemistry	130000 $/g
Terrylene	BLD Pharm	9240 $/g
TER-C8	**This Work**	**61.5 $/g**

Characterization:

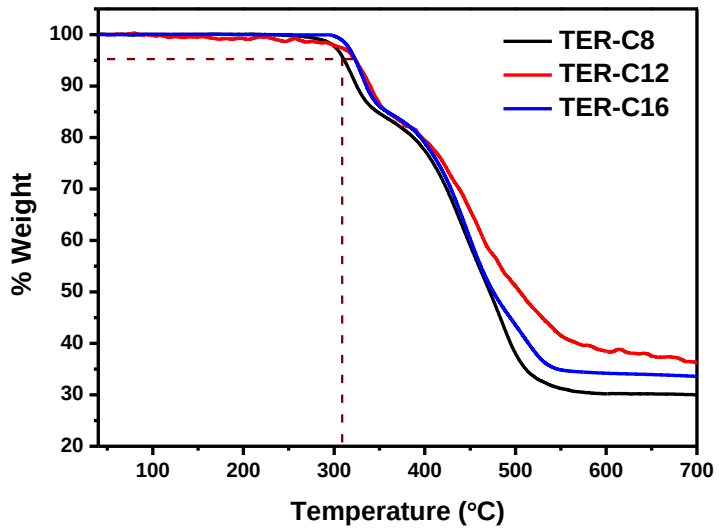

Fig. S14. Thermogravimetric analysis plot of **TER-C8**, **TER-C12** and **TER-C16**.

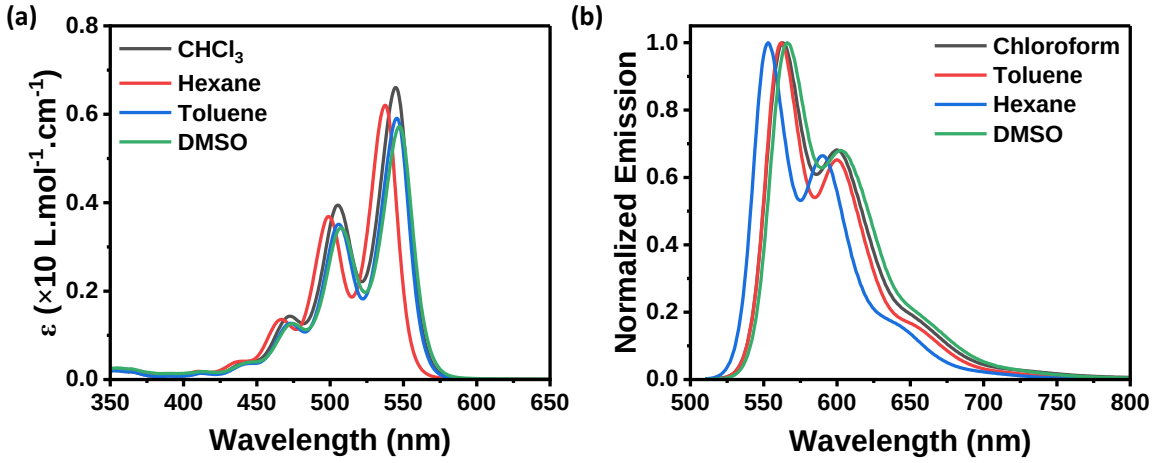

Fig. S15. (a) UV-vis and (b) fluorescence emission spectra of **TER-C8** in different solvents (10 μM).

Table S6. Absorption and emission maxima of **TER-C8** in different solvents.

	Chloroform	**Hexane**	**Toluene**	**DMSO**
λ_{abs}^{max} **(nm)**	544	537	545	547
λ_{em}^{max} **(nm)**	563	553	562	566

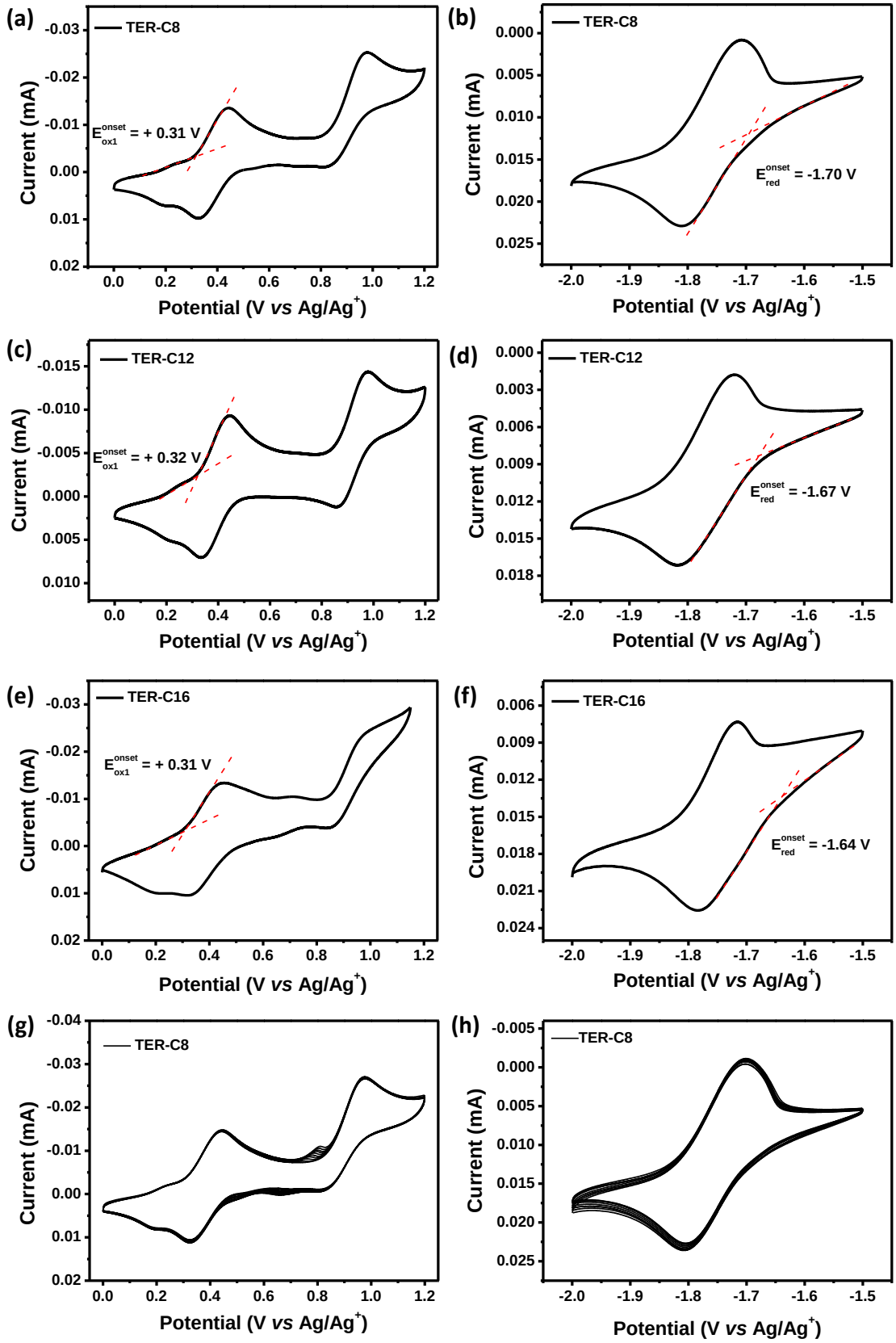

Fig. S16. Cyclic Voltammograms of **TER-C8** (a, b), **TER-C12** (c, d), **TER-C16** (e, f) and the electrochemical stability of **TER-C8** (g, h).

Table S7. Redox properties and energy levels of as synthesized 7,8-bis(alkyloxy)terrylenes.

	E_{onset}^{ox}(V)	E_{onset}^{red}(V)	E_{HOMO}^{CV}(eV)	E_{LUMO}^{CV}(eV)	E_{g}^{CV}(eV)
TER-C8	+0.31	-1.70	-5.19	-3.18	2.01
TER-C12	+0.32	-1.67	-5.20	-3.21	1.99
TER-C16	+0.31	-1.64	-5.19	-3.24	1.95

Thermal Properties

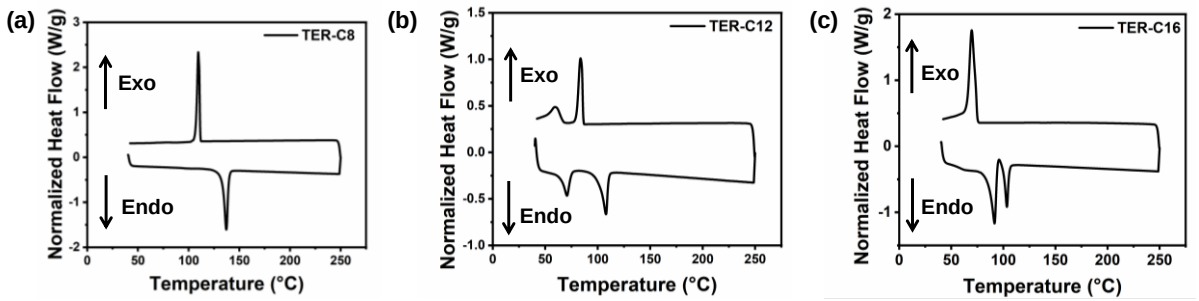

Fig. S17. Differential scanning calorimetry (DSC) thermograms of (a) **TER-C8**, (b) **TER-C12** and (c) **TER-C16**.

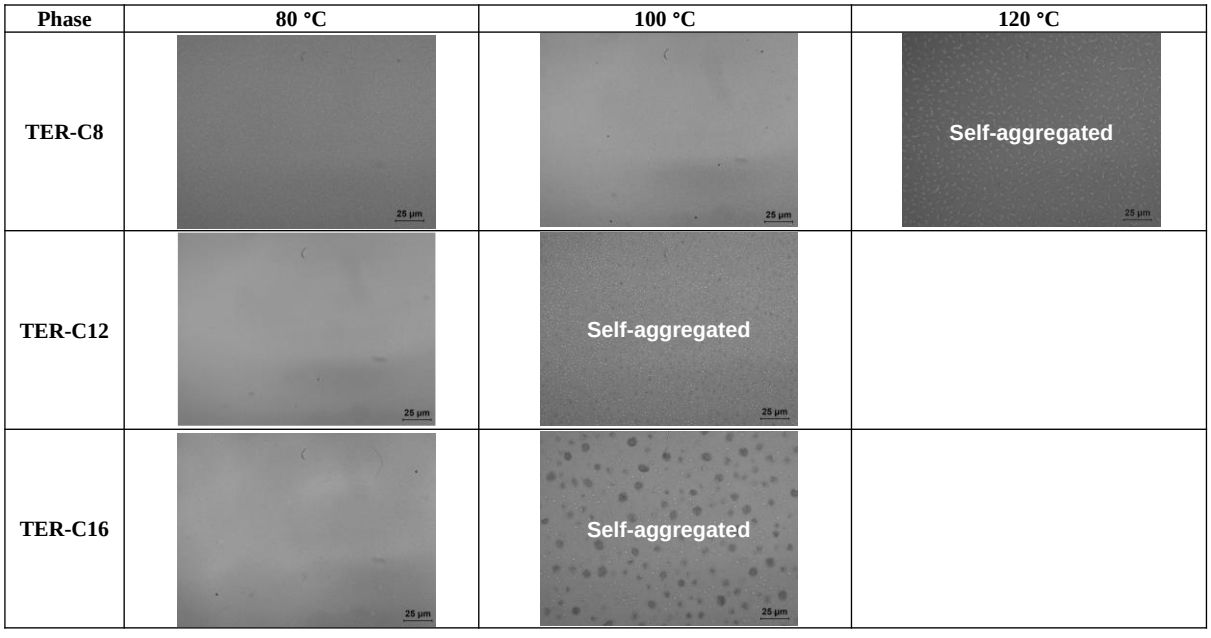

Fig. S18. Optical microscope images of the small molecules with different annealing temperatures.

Phase	TER-C8	TER-C12	TER-C16
50 °C annealed	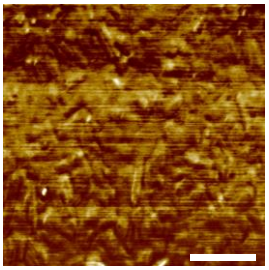	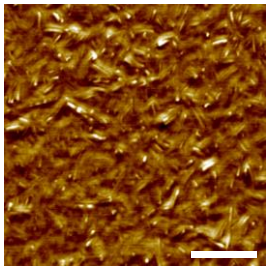	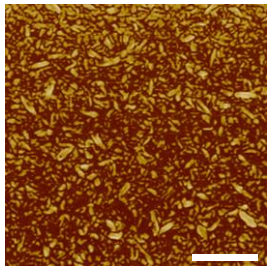
Annealing at optimized temperature	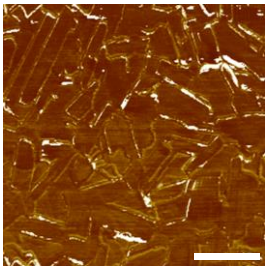	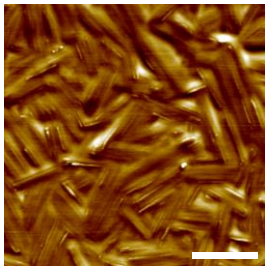	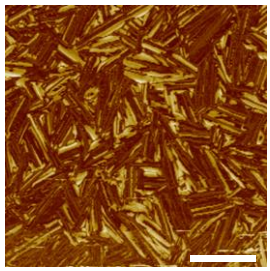

Fig. S19. AFM phase images of the small molecules after low and optimized temperature annealing. Scale bars, 500 nm.

Table S8. Hole mobilities during optimization of thermal annealing temperature.

Annealing Temperature (°C)	TER-C8			TER-C12			TER-C16		
	$\mu_{h,avg}$ ($cm^2 V^{-1} s^{-1}$)	I_{on}/I_{off}	V_{th} (V)	$\mu_{h,avg}$ ($cm^2 V^{-1} s^{-1}$)	I_{on}/I_{off}	V_{th} (V)	$\mu_{h,avg}$ ($cm^2 V^{-1} s^{-1}$)	I_{on}/I_{off}	V_{th} (V)
50	8.1×10^{-4}	3.4×10^{3}	-7.7	8.7×10^{-5}	8.1×10^{3}	-1.3	1.1×10^{-5}	1.8×10^{3}	12.4
80	1.5×10^{-3}	2.8×10^{4}	-4.8	3.5×10^{-4}	1.5×10^{4}	-2.2	3.6×10^{-5}	2.9×10^{3}	-6.9
100	3.0×10^{-3}	4.9×10^{5}	-10.1	1.5×10^{-4}	5.3×10^{5}	-6.3	-	-	-
120	1.1×10^{-3}	3.6×10^{4}	-18.4	-	-	-	-	-	-

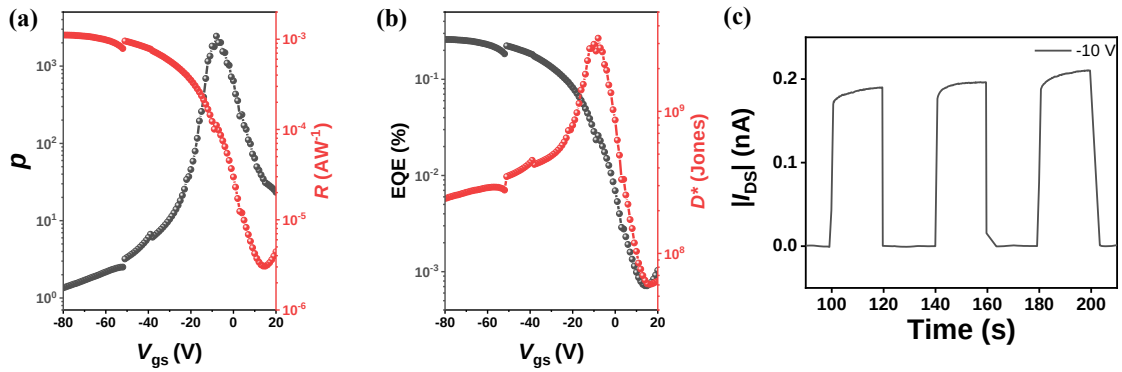

Fig. S20. (a) Photosensitivity, responsivity, (b) EQE and detectivity of **TER-C12** as a function of the gate voltage. (c) Time-dependent photoresponse characteristics of **TER-C12** under periodic dark and light illumination conditions.

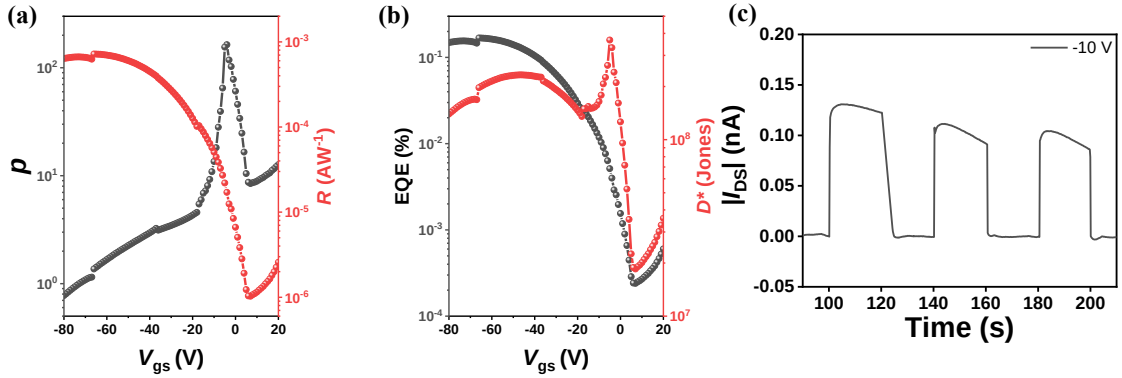

Fig. S21. (a) Photosensitivity, responsivity, (b) EQE and detectivity of **TER-C16** as a function of the gate voltage. (c) Time-dependent photoresponse characteristics of **TER-C16** under periodic dark and light illumination conditions.

Table S9. Summary of optoelectronic characteristics (p, R, EQE and D^*) of the small molecules. V_{ds} = -80 V.

	TER-C8	**TER-C12**	**TER-C16**
p_{MAX}	2.5×10^4	2.4×10^3	1.6×10^2
R_{MAX} (A/W)	1.5×10^{-2}	1.1×10^{-3}	7.2×10^{-4}
EQE_{MAX} (%)	3.6	0.26	0.17
D^*_{MAX} (Jones)	2.1×10^{10}	3.3×10^9	3.7×10^8

Reference.

1. Y. Wang, Q. Liao, J. Chen, W. Huang, X. Zhuang, Y. Tang, B. Li, X. Yao, X. Feng, X. Zhang, M. Su, Z. He, T. J. Marks, A. Facchetti and X. Guo, Teaching an Old Anchoring Group New Tricks: Enabling Low-Cost, Eco-Friendly Hole-Transporting Materials for Efficient and Stable Perovskite Solar Cells, *J. Am. Chem. Soc.*, 2020, **142**, 16632-16643.
2. A. D. Becke, Density-functional thermochemistry. I. The effect of the exchange-only gradient correction, *J. Chem. Phys.*, 1992, **96**, 2155-2160.
3. C. Lee, W. Yang and R. G. Parr, Development of the Colle-Salvetti correlation-energy formula into a functional of the electron density, *Phys. Rev. B.*, 1988, **37**, 785-789.
4. M. J. Frisch, G. W. Trucks, H. B. Schlegel, G. E. Scuseria, M. A. Robb, J. R. Cheeseman, G. Scalmani, V. Barone, G. A. Petersson, H. Nakatsuji, X. Li, M. Caricato, A. V. Marenich, J. Bloino, B. G. Janesko, R. Gomperts, B. Mennucci, H. P. Hratchian, J. V. Ortiz, A. F. Izmaylov, J. L. Sonnenberg, Williams, F. Ding, F. Lipparini, F. Egidi, J. Goings, B. Peng, A. Petrone, T. Henderson, D. Ranasinghe, V. G. Zakrzewski, J. Gao, N. Rega, G. Zheng, W. Liang, M. Hada, M. Ehara, K. Toyota, R. Fukuda, J. Hasegawa, M. Ishida, T. Nakajima, Y. Honda, O. Kitao, H. Nakai, T. Vreven, K. Throssell, J. A. Montgomery Jr., J. E. Peralta, F. Ogliaro, M. J. Bearpark, J. J. Heyd, E. N. Brothers, K. N. Kudin, V. N. Staroverov, T. A. Keith, R. Kobayashi, J. Normand, K. Raghavachari, A. P. Rendell, J. C. Burant, S. S. Iyengar, J. Tomasi, M. Cossi, J. M. Millam, M. Klene, C. Adamo, R. Cammi, J. W. Ochterski, R. L. Martin, K. Morokuma, O. Farkas, J. B. Foresman and D. J. Fox, Gaussian 16 Rev. C.01.*Journal*, 2016.
5. R. Dennington, T. Keith and J. Millam, GaussView, version 5, 2009.
6. S. K. Samanta, G. S. Kumar, U. K. Ghorai, U. Scherf, S. Acharya and S. Bhattacharya, Synthesis of High Molecular Weight 1,4-Polynaphthalene for Solution-Processed True Color Blue Light Emitting Diode, *Macromolecules*, 2018, **51**, 8324-8329.
7. L.-P. Yang, F. Jia, Q.-H. Zhou, F. Pan, J.-N. Sun, K. Rissanen, L. W. Chung and W. Jiang, Guest-Induced Folding and Self-Assembly of Conformationally Adaptive Macrocycles into Nanosheets and Nanotubes, *Chem. Eur. J.*, 2017, **23**, 1516-1520.